Strongly correlated multilayered nanostructures near the Mott transition

J. K. Freericks[*]

Department of Physics, Georgetown University, Washington, DC 20057, U.S.A.

We examine devices constructed out of multilayered sandwiches of semi-infinite metal–barrier–semi-infinite metal, with the barrier tuned to lie near the quantum critical point of the Mott metal-insulator transition. By employing dynamical mean field theory, we are able to solve the many-body problem exactly (within the local approximation) and determine the density of states through the nanostructure and the charge transport perpendicular to the planes. We introduce a generalization of the Thouless energy that describes the crossover from tunneling to incoherent thermally activated transport.

1 Introduction Many new technological developments are anticipated over the coming years in the field of nanotechnology. There is a current interest in trying to incorporate strongly correlated materials into nanoscale devices, because strongly correlated systems often have interesting bulk properties that can be tuned by changing the pressure, temperature, chemical doping, etc. What is lesser known is how the strong electron correlations are modified when the bulk materials are confined on the quantum scale and attached to other (noncorrelated) materials, like normal metallic leads. In particular, we expect there to be a reorganization of the electronic states driven by a charge transfer, associated with the mismatch of the chemical potentials, and by the normal-state proximity effect of the metallic leads on the insulator, which will produce exponentially decaying states within the barrier of the Mott insulator, analogous to the superconducting proximity effect in normal metals. Here we adjust our system to be overall charge neutral, so we do not investigate the charge transfer; we only investigate the proximity effect.

From a device standpoint, the simplest type of nanostructure to create is a multilayered structure, where stacks of planes of one material are topped by another material, and so on until a given device and heterostructure is made. Recent advances in pulsed laser deposition and molecular beam epitaxy have allowed many complex structures to be grown, with interfaces between the different materials being well defined up to a few atomic layers.

The question we will address in this contribution is how do the properties of semi-infinite metal–barrier–semi-infinite metal multilayered heterostructure vary with the barrier thickness when the barrier is a Mott insulator, tuned to lie just slightly above the Mott metal-insulator transition (i.e. very close to the quantum-critical point, but on the insulating side). We examine both single-particle properties like the density of states (DOS), including a proof that the local DOS in the barrier of a single-plane barrier has metallic behavior at strong coupling. We also investigate transport, and discuss a generalization of the Thouless energy that is appropriate for Mott-insulating systems and governs the crossover from tunneling to incoherent transport. We employ dynamical mean field theory (DMFT) to perform these calculations, which relies on the local approximation for the self energy to be accurate in these three-dimensional inhomogeneous systems.

[*] Corresponding author: e-mail: freericks@physics.georgetown.edu, Phone: +202 687 6179, Fax: +202 687 2087
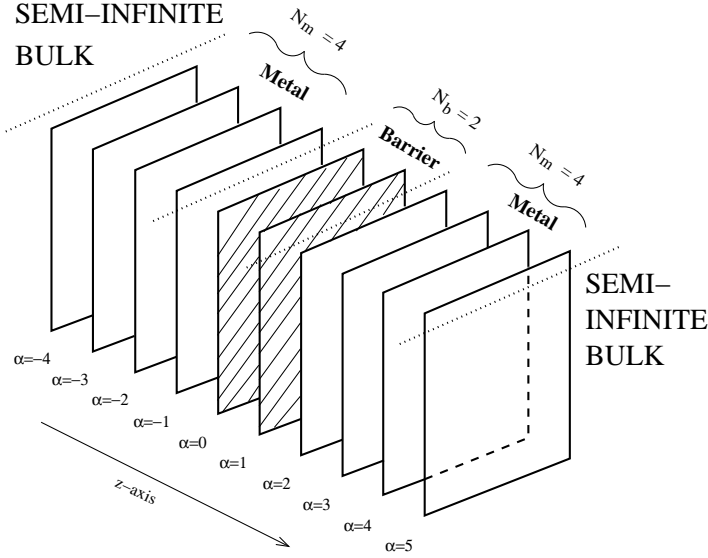
Fig. 1 Schematic of the multilayered nanostructure, where we take a finite number of self-consistent metal planes ($N_m = 4$ in the figure, but $N_m = 30$ in our calculations), couple them on one end to a bulk semi-infinite metal, and on the other end to a barrier described by the Falicov-Kimball model (with $N_b = 2$ in the figure depicted by the cross-hatched planes; in our calculations $N_b = N$ varies from 1 to 30).

2 Formalism

We describe the Mott insulator by the spinless Falicov-Kimball model [1]

$$\mathcal{H} = -\sum_{ij} t_{ij} c_i^\dagger c_j + \sum_i U_i \left(c_i^\dagger c_i - \frac{1}{2} \right) \left(w_i - \frac{1}{2} \right) \tag{1}$$

where t_{ij} is a Hermitian hopping matrix, U_i is the Falicov-Kimball interaction, and w_i is a classical variable that equals one if there is a localized particle at site i and zero if there is no localized particle at site i (a chemical potential μ is employed to adjust the conduction-electron concentration). Since we are considering multilayered heterostructures (see Fig. 1), we assume that the hopping matrix is translationally invariant within each plane, as well as the Falicov-Kimball interaction. For simplicity, we will take the lattice sites to lie on the sites of a simple cubic lattice, with $t_{ij} = t$ for all nearest neighbors (we use t as our unit of energy), and we will take $U_i = U$ for all lattice sites i that lie within the barrier plane. This choice assumes that the bare kinetic energy is the same for the metallic leads and for the barrier, and that the barrier is strongly correlated via the Falicov-Kimball interaction (renormalizing its bandstructure) within the barrier planes. We also work at half filling, with $\mu = 0$ and $\langle w_i \rangle = w_1 = 1/2$. In this case, the chemical potential has no temperature dependence, and the electronic charge remains homogeneous throughout the system.

The dynamical mean field theory for inhomogeneous systems was originally worked out by Potthoff and Nolting [2] and developed for these particular heterostructures in another publication [3]. Here we just include the relevant summarizing formulas. The starting point is to note that the system has translational invariance in the two-dimensional planar direction, so we can Fourier transform from real space to momentum space; all physical quantities we will be interested in here depend only on the two-dimensional bandstructure $\epsilon^{2d} = -2t[\cos \mathbf{k}_x + \cos \mathbf{k}_y]$. We let a Greek letter (α, β, γ, ...) denote the z-component of each of the stacked planes. Then, because an electron with energy ϵ^{2d} in the perpendicular direction, decouples from electrons with different perpendicular energy, the problem for the Green's function reduces to a quasi-one-dimensional problem, that can be solved with the renormalized perturbation expansion [4].

The result for the local retarded Green's function at plane α is

$$G_\alpha(\omega) = \int d\epsilon^{2d} \rho^{2d}(\epsilon) \frac{1}{L_\alpha(\epsilon^{2d}, \omega) + R_\alpha(\epsilon^{2d}, \omega) - [\omega + \mu - \Sigma_\alpha(\omega) - \epsilon^{2d}]} \qquad (2)$$

with ρ^{2d} the DOS of a two-dimensional tight-binding square lattice and $\Sigma_\alpha(\omega)$ the self energy at plane α. The functions R and L are determined via recursion relations:

$$R_{\alpha+n}(\epsilon^{2d}, \omega) = \omega + \mu - \Sigma_{\alpha+n}(\omega) - \epsilon^{2d} - \frac{1}{R_{\alpha+n+1}(\epsilon^{2d}, \omega)}; \qquad (3)$$

$$L_{\alpha-n}(\epsilon^{2d}, \omega) = \omega + \mu - \Sigma_{\alpha-n}(\omega) - \epsilon^{2d} - \frac{1}{L_{\alpha-n-1}(\epsilon^{2d}, \omega)}; \qquad (4)$$

for $n > 0$. These recurrences are solved by starting at $n = \pm\infty$ for the right or left recurrence, and then iterating in n. Of course, in real calculations, we must assume $R_\alpha = R_\infty$ and $L_\alpha = L_{-\infty}$ for all α up to a finite distance away from the interfaces with the barriers; we include 30 such self-consistent planes in the metallic leads (on each side of the barrier) in our calculations. We determine R_∞ ($L_{-\infty}$) by substituting R_∞ ($L_{-\infty}$) into both the left and right hand sides of Eq. (3) [Eq. (4)], which produces a quadratic equation that is solved by

$$R_\infty(\epsilon^{2d}, \omega) = \frac{\omega + \mu - \Sigma_{bulk}(\omega) - \epsilon^{2d}}{2} \pm \frac{1}{2}\sqrt{[\omega + \mu - \Sigma_{bulk}(\omega) - \epsilon^{2d}]^2 - 4} = L_{-\infty}(\epsilon^{2d}, \omega), \quad (5)$$

with the sign of the square root chosen by analyticity or continuity. In both Eqs. (3) and (4), we see that whenever the imaginary part of R or L is positive, it remains positive in the recursion, implying stability; similarly, when the imaginary part is zero, we find the large root is stable, which is the physical root. Hence the recurrences are stable.

Once we have determined the local Green's function on each plane, we can perform the DMFT calculation to determine the local self energy on each plane [5, 6]. We start with Dyson's equation, which defines the effective medium for each plane

$$G_{0\alpha}^{-1}(\omega) = G_\alpha^{-1}(\omega) + \Sigma_\alpha(\omega). \qquad (6)$$

The local Green's function for the αth plane satisfies

$$G_\alpha(\omega) = (1 - w_1)\frac{1}{G_{0\alpha}^{-1}(\omega) + \frac{1}{2}U} + w_1\frac{1}{G_{0\alpha}^{-1}(\omega) - \frac{1}{2}U}, \qquad (7)$$

with w_1 equal to the average filling of the localized particles [note that this above form is slightly different from the usual notation [6], because we have made the theory particle-hole symmetric by the choice of the interaction in Eq. (1), so that $\mu = 0$ corresponds to half filling in the barrier region and in the ballistic metal leads]. Finally, the self energy is found from

$$\Sigma_\alpha(\omega) = G_{0\alpha}^{-1}(\omega) - G_\alpha^{-1}(\omega). \qquad (8)$$

The full DMFT algorithm begins by (i) making a choice for the self energy on each plane. Next, we (ii) use the left and right recurrences in Eqs. (3) and (4) along with the bulk values found in Eqs. (5) and the 30 self-consistently determined planes within the metal leads to calculate the local Green's function at each plane in the self-consistent region from Eq. (2). Once the local Green's function is known for each plane, we then (iii) extract the effective medium for each plane from Eq. (6), (iv) determine the new local Green's function from Eq. (7), and (v) calculate the new self energy on each plane from Eq. (8). Then we iterate through steps (ii)–(v) until the calculations have converged.

3 Numerical results   The first thing we consider is the local DOS on the barrier plane for a single-plane barrier ($N = 1$) in Fig. 2 (a). Note how the DOS looks like a Mott insulator for large U (in the bulk, the Mott transition occurs at $U \approx 4.9$), with an upper and lower Hubbard band forming, but there is substantial low-energy DOS coming from the interface localized states that are actually metallic in character (negative second derivative of the DOS with respect to ω). In addition, we show the Friedel-like oscillations that develop in the metallic leads as we move away from the barrier interface (for $U = 5$) in Fig. 2 (b). Note how the oscillations have a shorter period, and a smaller amplitude as we move away from the interface. Already at 10 lattice spacings away from the interface, we see there is only a small difference from the bulk DOS (which is why 30 self-consistent planes is sufficient for this work).
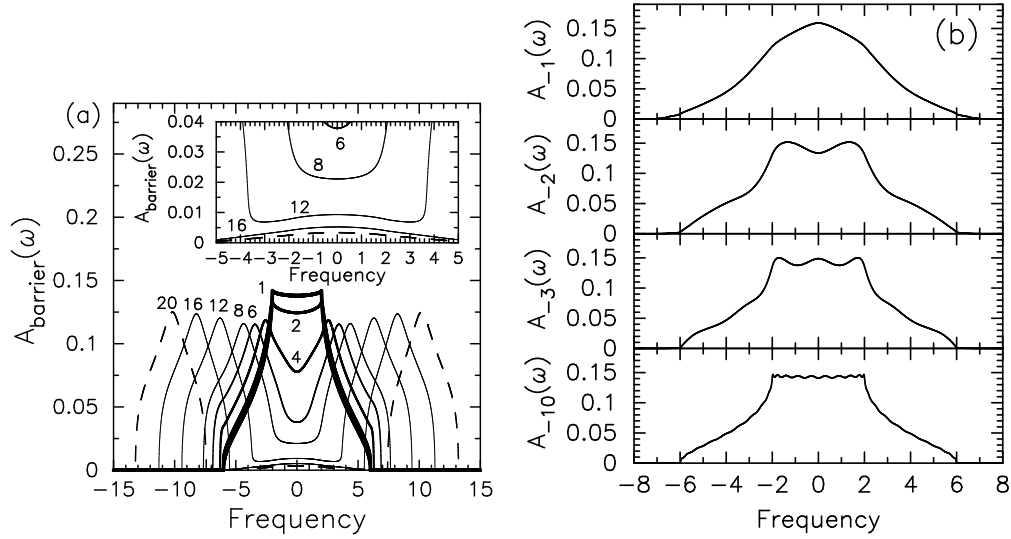

Fig. 2 (a) Local DOS for the barrier plane when $N = 1$ and for various U (indicated by the numerical labels). The inset highlights the low-energy region, where one can see a low-weight metallic DOS form for large U from the interface localized states of the nanostructure. (b) The local DOS in four barrier planes for $U = 5$ and $N = 5$ (the first barrier plane is at $\alpha = 0$; the metallic lead runs from $\alpha = -1$ to $\alpha = -30$ on the left hand side). Note how the amplitude of the Friedel-like oscillations are quite small even by the time we hit the tenth plane from the barrier.

We show that the peak value at $\omega = 0$ is easy to derive from an analysis of the Potthoff-Nolting algorithm, and that it is nonvanishing for all U. To begin, we consider the non-self-consistent solution, where we set $L_\alpha = L_{-\infty}$ and $R_\alpha = R_\infty$ for all α except $\alpha = 0$, where we have a Falicov-Kimball interaction. Then the local Green's function in the barrier is

$$G_{\alpha=0}(\omega) = \int d\epsilon \rho^{2d}(\epsilon) \frac{1}{2(\omega + \frac{1}{2}U - \epsilon) - \Sigma_0(\omega) \pm \sqrt{(\omega - \epsilon)^2 - 4}}, \tag{9}$$

where the sign of the square root is chosen by either analyticity, or continuity. If we assume Σ_0 is large (which occurs in the Mott insulator) then we can expand Eq. (9) in a power series in inverse powers of Σ to give

$$G_{\alpha=0}(\omega) \approx -\frac{1}{\Sigma_0(\omega)} - \frac{2\omega + U \pm s(\omega)}{\Sigma_0^2(\omega)} + \dots \tag{10}$$

with $s(\omega) = \int \rho^{2d}(\epsilon) \sqrt{(\omega + \frac{1}{2}U - \epsilon)^2 - 4}$. Taking the value for $G_{\alpha=0}$ from Eq. (10), and plugging it into the self-consistent DMFT algorithm described above, allows us to solve for the self energy directly,

with the result

$$\Sigma_0(\omega) = \frac{\frac{1}{4}U^2}{2\omega + U \pm s(\omega)} \tag{11}$$

which is large for $U \gg 1$, consistent with our ansatz. If we perform the integral in the definition of $s(\omega)$, we find it satisfies $s(\omega) = (\omega + \frac{1}{2}U) \cdot 0.653 + i \cdot 1.05$. Substituting this result into the self energy, and then into the Green's function, and evaluating the DOS, finally yields

$$\rho_0(\omega) \approx \frac{1.05}{\pi[(1.05^2 + \frac{1}{4}U^2]}; \tag{12}$$

we compare this result to the exact calculated result in Table 1. One can see the agreement is excellent.

Table 1 Comparison of the results from Eq. (12) and the exact numerical DOS for a single-plane barrier and various U.

U	approximate result [Eq. (12)]	exact numerical result
6	0.033	0.037
8	0.0195	0.021
12	0.009	0.009
16	0.005	0.005
20	0.003	0.003

In Fig. 3, we plot a false color (grayscale) plot of the DOS of the nanostructure in the near critical region $U = 5$ for a moderately thick ($N = 20$) barrier. Note how the Friedel oscillations are most apparent in the center of the band in the metallic leads (upper part of the graph). We only plot the 40 planes on the left-hand-side of the nanostructure, because the symmetry of the structure guarantees the rest of the nanostructure can be determined by a mirror plane reflection. Note how there are few oscillations within the barrier itself, and how the DOS rapidly becomes small at low energy (because it is an insulator). It is possible to even see some oscillations induced in the metallic lead at energies close to the band edge, and at positions close to the interface.

We examine transport properties in Fig. 4. The resistance of a junction is calculated in the linear-response regime via a Kubo-based formalism [7] with the current-current correlation function [8, 3]. The formalism requires us to employ a conductivity matrix in real space, with matrix components corresponding to the z-axis label of the different planes in the system. The resistance-area product can be calculated for any temperature.

We extract an energy scale from the resistance, which we call the Thouless energy [9, 10], since it reduces to the well-known diffusive and ballistic limits, but it also defines an energy scale when the barrier is a Mott insulator. In the insulating phase, it is a function of time, and the point where $E_{Th} \approx T$ defines an important energy scale for the dynamics of the transport in a nanostructure—it signifies when the transport crosses over from tunneling behavior at low T to incoherent "Ohmic" transport at high T [see Fig. 4 (a)]. On the other hand, the Thouless energy is inversely proportional to L, the thickness of the barrier for ballistic transport and inversely proportional to L^2 for diffusive transport [this can be seen from taking the low-temperature limit of Eq. (13) and noting that the DOS is nearly constant near the Fermi energy at low temperature and recalling the $R_n \propto L$ for diffusive transport and R_n is independent of L for ballistic transport].

The generalized formula for the Thouless energy is [11, 3]

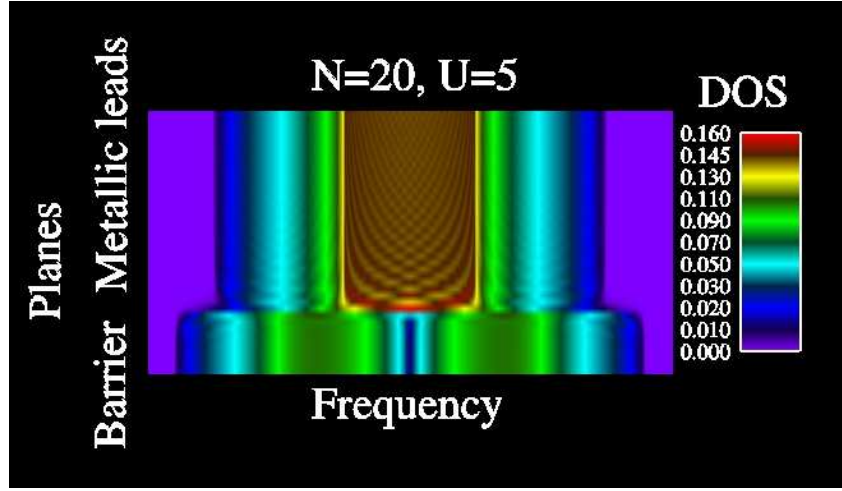$$E_{Th} = \frac{\hbar}{R_n a^2 2e^2 \int d\omega [-df/d\omega] \rho_{bulk}(\omega) L}, \tag{13}$$

Fig. 3 False color (grayscale) plot of the local DOS for the near critical $U = 5$ nanostructure with $N = 20$ planes in the barrier. Note how the Friedel oscillations in the metallic lead are most apparent near the center of the band, and how there are limited oscillations in the barrier (the DOS decays exponentially fast with position in the barrier at low energy). (Color on-line.)
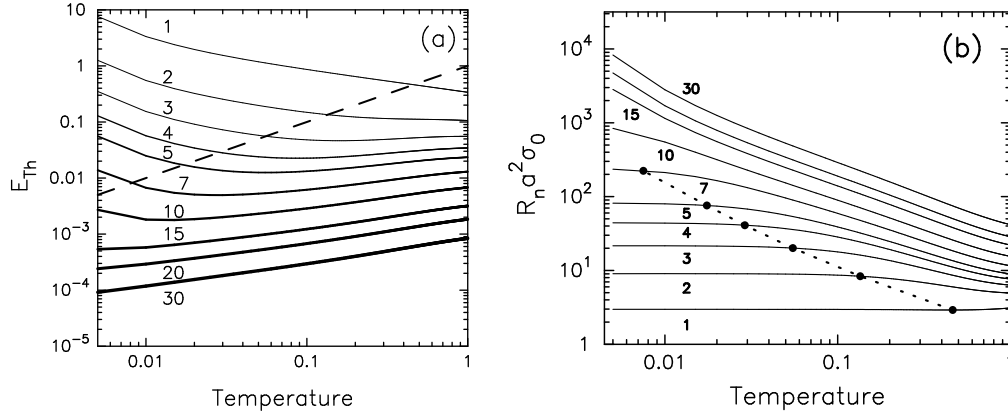

Fig. 4 (a) Thouless energy for the $U = 5$ nanostructure as a function of temperature on a log-log plot. The different curves are for different thicknesses of the barrier. The dashed line is the curve $E_{Th} = T$, and the special points that denote the crossover from tunneling to incoherent transport correspond to the points of intersection of the solid lines with the dashed line. (b) Resistance-area product plotted versus the temperature on a log-log plot. The different curves correspond to different barrier thicknesses. The solid dots and the dotted line plots the points where $E_{Th} = T$. Note how the curves are flat at low temperature and for thin junctions indicating tunneling (but the tunneling resistance does not grow exponentially with the thickness when we are so close to the metal-insulator transition and at finite temperature–note the unequal spacing of the lines with N). At higher temperature, the resistance picks up strong temperature dependence, and the transport is best described by incoherent thermally activated processes. The numerical labels on the figures denote the thickness of the barrier of the nanostructure and the constant satisfies $\sigma_0 = 2e^2/ha^2$.

where a is the lattice spacing, e is the electrical charge, $\hbar$ is Planck's constant, R_n is the junction resistance, $f(\omega) = 1/[1 + \exp(\omega/T)]$ is the Fermi-Dirac distribution, ρ_{bulk} is the interacting bulk DOS of the barrier material, and $L = Na$ is the thickness of the barrier.

The resistance-area product versus temperature is plotted in Fig. 4 (b). Note the flat regions for low T and thin junctions. This is a signal that the transport is dominated by tunneling, but because the gap is so small in this system, we do not see an exponential increase in the resistance-area product with the thickness of the junction. Instead, it increases with a functional behavior in between that of an exponential increase and of a linear increase. We also include a plot of the points where the Thouless energy is equal to the temperature. In this case, they are close to, but not exactly at the point where the tunneling behavior crosses over to incoherent transport (which has a strong temperature dependence). As U is increased further, this separation becomes more readily apparent [3]. We believe this anomalous behavior occurs because the system is so close to the critical point of the metal-insulator transition,

4 Conclusions In this contribution we examined properties of a nanostructure composed of metallic leads and a barrier that could be tuned through the metal-insulator transition (described by the Falicov-Kimball model). We concentrated on general properties of the thin barrier (where we showed it always has a metallic DOS generated by the normal proximity effect with the metallic leads, although the weight within this metallic "subband" can be quite small). We also investigated the DOS and transport properties of a near critical Mott insulating barrier with $U = 5$ (the critical value of the transition on a simple cubic lattice is $U_c \approx 4.9$ within DMFT). We found the system shows behavior that looks like tunneling, but it also has a number of anomalies, the most important being that the resistance does not grow exponentially with the junction thickness in the tunneling regime. We also defined a generalization of the Thouless energy that reduces to the ballistic and diffusive limits, but can also describe strongly correlated insulators. We found the Thouless energy picks up strong temperature dependence in this regime and the point where $E_{Th} = T$ determines an approximate crossover from tunneling to incoherent transport, where the resistance is proportional to the bulk resistivity of the barrier multiplied by some geometrical factors (and the resistivity has strong exponentially activated behavior in T for a correlated insulator).

There are a number of future directions that are important to consider as one tries to examine models closer to experimental systems. First, there will be a charge transfer (electronic charge reconstruction) [12, 13] when the chemical potentials do not match, which can have strong effects on correlated systems, especially correlated insulators, second, it is useful to consider capacitive effects for these devices, since the junction capacitance will play a role in the switching speed, and third, it would be interesting to extend this analysis from equilibrium/linear response to nonequilibrium/nonlinear response, where one could directly calculate the current-voltage characteristic of the device, and determine the origins of its nonlinearities.

References

[1]   L. M. Falicov and J. C. Kimball, Phys. Rev. Lett. **22**, 997 (1969).
[2]   M. Potthoff and W. Nolting, Phys. Rev. B **59**, 2549 (1999).
[3]   J. K. Freericks, submitted to Phys. Rev. B.
[4]   E. N. Economou, *Green's Functions in Quantum Physics*, (Springer-Verlag, Berlin, 1983).
[5]   U. Brandt and C. Mielsch, Z. Phys. B **75**, 365 (1989).
[6]   J. K. Freericks and V. Zlatić, Rev. Mod. Phys. **75**, 1333 (2003).
[7]   R. Kubo, J. Phys. Soc. Japan, **12**, 570 (1957).
[8]   P. Miller and J. K. Freericks, J. Phys.: Condens. Matt. **13**, 2354 (2001).
[9]   J. T. Edwards and D. J. Thouless, J. Phys. C **5**, 807 (1972).
[10] D. J. Thouless, Phys. Rep. **13**, 93 (1974).
[11] J. K. Freericks, Appl. Phys. Lett. **84**, 1383 (2004).
[12] B. N. Nikolić, J. K. Freericks, and P. Miller, Phys. Rev. B **65**, 064529 (2002).
[13] S. Okamoto and A. J. Millis, Nature **428**, 630 (2004).